Muffin tin orbitals of arbitrary order

O.K. Andersen, T. Saha-Dasgupta, C. Arcangeli, R.W. Tank, G. Krier, O. Jepsen and E. Pavarini

Introduction: For electrons in condensed matter, it is often desirable to express the single-particle wave functions, $\Psi_i(\mathbf{r})$, with energies ε_i in a certain range in terms of a minimal set of state- and energy-independent orbitals, $\chi_{RL}(\mathbf{r})$. Here, R spans the sites, and L the local symmetry (e. g. $L{\equiv}lm$). A few examples: *(a)* In a crystal, the electrons belonging to an energy band which does not overlap any other band are most simply described in terms of the Wannier functions, $\chi(\mathbf{r}-\mathbf{R})$, with R spanning the lattice translations. *(b)* Model Hamiltonians are usually expressed in representations which for the electrons are assumed to be minimal and orthonormal. (c) In a density-functional calculation, the use of a minimal basis set for solving the Schrödinger equation self-consistently would ease the interpretation of the results and speed up the calculation. For realistic systems, however, it is hard to obtain a minimal basis of useful accuracy.

We have derived a general method for obtaining such minimal basis sets for cases where the wave functions are solutions of a Schrödinger equation which is locally separable,

$$\mathcal{H}\Psi_i(\mathbf{r}) \equiv [-\triangle + V(\mathbf{r})]\,\Psi_i(\mathbf{r}) = \varepsilon_i \Psi_i(\mathbf{r}), \tag{1}$$

specifically, where the potential has the muffin tin form: $V(\mathbf{r}) = \sum_R v_R(|\mathbf{r}-\mathbf{R}|)$. This work is part of an ongoing effort to develop an electronic-structure method which is generally applicable, intelligible, and computationally fast and accurate.

A MT potential divides space into MT spheres with radii a_{R}, where the potential is spherically symmetric, and a rest, the interstitial, where the potential is flat (zero). Inside each sphere and in the interstitial one may solve Schrödinger's differential equation (numerically) for an energy, ε, chosen in the range of interest. In case the resulting partial solutions, $\phi(\varepsilon,\mathbf{r})$, can be matched continuously and differentiably at the spheres, they form a wave function, $\Psi_i(\mathbf{r})$, with $\varepsilon_i{=}\varepsilon$. Such matching schemes (e. g. those of Wigner and Seitz and of Korringa, Kohn, and Rostoker (KKR)) are not very practical, however. Instead, we want to use the $\phi(\varepsilon,\mathbf{r})$'s to construct a set of energy-independent orbitals, $\chi^{(N)}(\mathbf{r})$, which span any wave function with energy ε_i in the neighborhood of N + 1 chosen energies, $\epsilon_0, ..., \epsilon_N$, to within an error proportional to $(\varepsilon_i-\epsilon_0)...(\varepsilon_i-\epsilon_N)$. Specifically, if the energy mesh is condensed onto one energy, ϵ_0, the error of a wave function with energy ε_i will be proportional to $(\varepsilon_i-\epsilon_0)^{\mathrm{N}+1}$. These orbitals we call Nth-order muffin tin orbitals, or NMTOs. Note that N does not influence the size of the NMTO basis set, but the range of the individual orbitals. Let us now work this out in more detail.

Kinked partial waves: Inside the sphere at $\mathbf{R}$, the partial solutions are $\varphi_{Rl}(\varepsilon,|\mathbf{r}-\mathbf{R}|)\,Y_L\left(\widehat{\mathbf{r}-\mathbf{R}}\right) \equiv \varphi_{Rl}(\varepsilon,r_R)\,Y_L(\hat{r}_R)$, where the energy-dependent function is the regular solution of the radial Schrödinger equation. In the interstitial region, we use those solutions of the wave equation, $(\triangle+\varepsilon)\,\psi_{RL}(\varepsilon,\mathbf{r})=0$, which satisfy the following homogeneous boundary condition: The projection of $\psi_{RL}(\varepsilon,\mathbf{r})$ onto $\delta(r_{R'}-a_{R'})\,Y_{L'}(\hat{r}_{R'})$ is $\delta_{RR'}\delta_{LL'}$. As an example, $\psi_{RL}(\varepsilon{=}0,\mathbf{r})$ is the electrostatic potential from a 2^l multipole centered at $\mathbf{R}$ when all other spheres are grounded. The

$\psi_{RL}(\varepsilon, \mathbf{r})$'s are called *screened spherical waves*. In fact, only those with RL corresponding to the so-called *active* channels will be used, and only the projections onto other active channels vanish. For the projection of the screened spherical wave onto an *in*active channel, the radial logarithmic derivative equals that of the solution to the radial *Schrödinger* equation. We can now form the set of so-called *kinked partial waves:* The kinked partial wave, $\phi_{RL}(\varepsilon, \mathbf{r})$, is $\varphi_{Rl}(\varepsilon, r_R) Y_L(\hat{r}_R)$ inside its own sphere and for its own angular momentum. It is $\psi_{RL}(\varepsilon, \mathbf{r})$ in the interstitial region and, inside the sphere at $\mathbf{R}'$, it vanishes for any other $(R'L' \neq RL)$ active channel, but it is proportional to $\varphi_{R'l'}(\varepsilon, r_{R'}) Y_{L'}(\hat{r}_{R'})$ for an inactive channel. As a result, $\phi_{RL}(\varepsilon, \mathbf{r})$ is continuous (we normalize the radial solutions of the active channels such that $\varphi_{Rl}(\varepsilon, a_R) \equiv 1$) and is a solution of Schrödinger's equation with energy ε. But it has kinks at the spheres in the active channels and is therefore *not* a wave function.

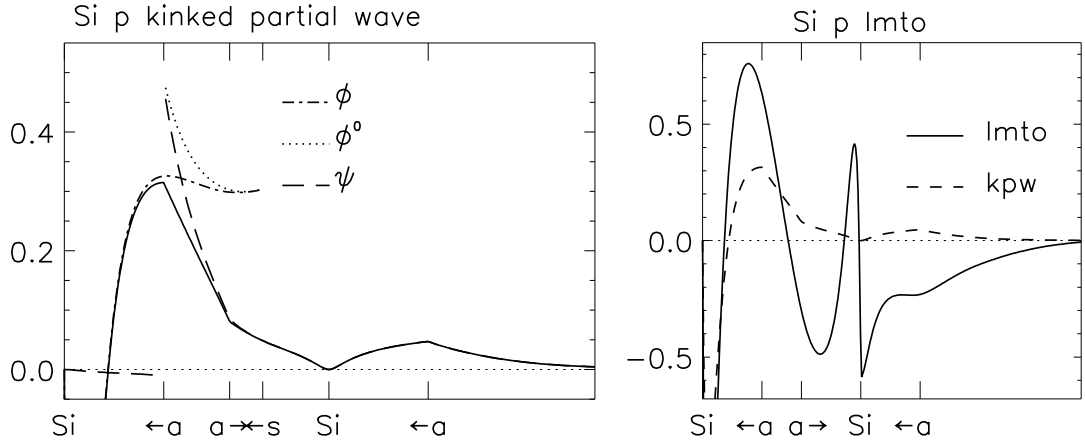

Figure 1: *Si $p_{x=y=z}$ kinked partial wave (KPW) and linear muffin tin orbital (LMTO).*

The solid curve in the left-hand part of Fig. 1 shows the Si $p_{x=y=z}$ kinked partial wave for ε in the middle of the valence band and for $\mathbf{r}$ along the [111]-line in the diamond structure from the central Si atom, through the nearest Si neighbor, and half-way into the back-bond void. The other curves will be explained later. The kinks at the a-spheres are clearly seen. Since this kinked partial wave is designed for use in a *minimal* sp^3-basis, only the Si s and p waves were chosen as active. The inactive partial waves – most notably Si d – must therefore be provided by the tails of the kinked partial waves centered at the neighbors, and this is the reason for the strong Si d-character seen inside the nearest-neighbor sphere. Had we been willing to keep Si d-orbitals in the basis, the Si d-channels would have been active so that only partial waves with $l > 2$ would have remained inside the neighbor spheres, whereby the kinked partial wave would have been more localized. Hence, the price for a smaller basis is a longer spatial range and a stronger energy dependence.

Kink matrix and matching equations: The central quantity of the present formalism is the Hermitian *kink matrix*, whose element $K_{R'L',RL}(\varepsilon)$ is defined to be the kink of $\phi_{RL}(\varepsilon, \mathbf{r})$ at the $a_{R'}$-sphere, projected onto $Y_{L'}(\hat{r}_{R'})/a_{R'}^2$. Hence, it specifies how the Hamiltonian (1) operates on the set of kinked partial waves:

$$(\mathcal{H} - \varepsilon)\, \phi_{RL}(\varepsilon, \mathbf{r}) = -\sum\nolimits_{R'L'} \delta(r_{R'} - a_{R'})\, Y_{L'}(\hat{r}_{R'})\, K_{R'L',RL}(\varepsilon)\,. \tag{2}$$

Although an individual kinked partial wave is not a wave function, any *smooth* linear combination, $\sum_{RL} \phi_{RL}(\varepsilon, \mathbf{r})\, c_{RL,i}$, is. Schrödinger's equation may therefore be formulated as the matching- or kink-cancellation condition:

$$\sum\nolimits_{RL} K_{R'L',RL}(\varepsilon_i)\, c_{RL,i} = 0 \quad \text{for all } R'L', \tag{3}$$

which is a set of homogeneous linear equations, equivalent with the KKR equations. Here, the indices run only over active channels. Since the kink-matrix is expensive to compute, it is not efficient to find a one-electron energy from $\det|K(\varepsilon_i)| = 0$, and then solve the linear equations for the corresponding $c_{RL,i}$, but to construct an energy- and state-independent basis set of NMTOs, and then solve the generalized eigenvalue problem,

$$\sum\nolimits_{RL} \left\langle \chi^{(N)}_{R'L'} \left| \mathcal{H} \right| \chi^{(N)}_{RL} \right\rangle c_{RL,i} \;=\; \varepsilon_i \sum\nolimits_{RL} \left\langle \chi^{(N)}_{R'L'} \mid \chi^{(N)}_{RL} \right\rangle c_{RL,i} \quad \text{for all } R'L', \tag{4}$$

resulting from the Raleigh-Ritz variational principle.

MTOs with N = 0: Since all wave functions with a certain energy may be expressed as linear combinations of the kinked partial waves with the *same* energy, the MTOs with N = 0 are simply the kinked partial waves at the chosen energy: $\chi^{(0)}_{RL}(\mathbf{r}) = \phi_{RL}(\epsilon_0, \mathbf{r})$. In the basis of these, the Hamiltonian and overlap matrices are given by respectively:

$$\left\langle \chi^{(0)} \left| \mathcal{H} - \epsilon_0 \right| \chi^{(0)} \right\rangle = -K(\epsilon_0) \quad \text{and} \quad \left\langle \chi^{(0)} \mid \chi^{(0)} \right\rangle = \dot{K}(\epsilon_0), \tag{5}$$

as may be found from Eq.(2) and the normalization. Here, $\dot{} \equiv \partial/\partial\varepsilon$. The energy solutions of the generalized eigenvalue problem (4) have errors proportional to the *square* of the wave-function errors, that is, $\propto (\varepsilon_i - \epsilon_0)^2$ when N = 0. This also follows trivially from the fact that Eqs.(4)–(5) are merely the energy-linearization of the matching equations (3).

Green matrix and MTOs with N > 0: In order to construct MTOs with N > 0, it is useful first to define a *Green matrix* as the inverse of the kink matrix: $G(\varepsilon) \equiv K(\varepsilon)^{-1}$. As seen from (3), its poles are the one-electron energies. Next, by an equation of the usual type: $(\mathcal{H} - \varepsilon)\, \gamma_{RL}(\varepsilon, \mathbf{r}) = -\delta(r_R - a_R)\, Y_L(\hat{r}_R)$, we define a Green function, $\gamma_{RL}(\varepsilon, \mathbf{r})$, which has one of its spatial variables confined to the a-spheres, i. e. $\mathbf{r}' \rightarrow RL$. Considered a function of $\mathbf{r}$, this confined Green function is a solution with energy ε of the Schrödinger equation, except at its own sphere and for its own angular momentum where it has a kink of size unity. This kink becomes negligible compared to the value of the function when ε is close to a one-electron energy because the Green function has a pole there. Equation (2) shows that $\gamma(\varepsilon, \mathbf{r}) = \phi(\varepsilon, \mathbf{r})\, G(\varepsilon)$. Here, and in the following, lower-case letters denote vectors and upper-case matrices (ε, ϵ, RL, and N are numbers, though). The confined Green function is thus factorized into a Green matrix, $G(\varepsilon)$, which has the full energy dependence, and a vector of functions, $\phi(\varepsilon, \mathbf{r})$, which has the full spatial dependence and a weak energy dependence. The kind of energy range we are considering is such that for two energies within the range, $\phi_{RL}(\varepsilon, \mathbf{r})$ and $\phi_{RL}(\varepsilon', \mathbf{r})$ are never orthogonal. Finally, we want to factorize the $\mathbf{r}$ and ε-dependencies completely and, hence, approximate the confined Green function by $\chi^{(N)}(\mathbf{r})\, G(\varepsilon)$. Subtracting from the Green function a function which is analytical in ε, obviously produces an equally good Green function, $\phi(\varepsilon, \mathbf{r})\, G(\varepsilon) - \omega^{(N)}(\varepsilon, \mathbf{r}) \equiv \chi^{(N)}(\varepsilon, \mathbf{r})\, G(\varepsilon)$, in the sense that both yield the same Schrödinger-equation solutions. If we can therefore determine

the vector of analytical functions in such a way that each $\chi_{RL}^{(N)}(\varepsilon,\mathbf{r})$ takes the *same* value, $\chi_{RL}^{(N)}(\mathbf{r})$, at all N + 1 energies, $\epsilon_0, ..., \epsilon_N$, then

$$\chi_{RL}^{(N)}(\varepsilon,\mathbf{r}) = \chi_{RL}^{(N)}(\mathbf{r}) + O\left((\varepsilon-\epsilon_0)...(\varepsilon-\epsilon_N)\right), \tag{6}$$

and, hence, $\chi^{(N)}(\mathbf{r})$ is the set of NMTOs. Now, since $\chi^{(N)}(\epsilon_0,\mathbf{r}) = ... = \chi^{(N)}(\epsilon_N,\mathbf{r})$, the Nth divided difference of $\chi^{(N)}(\varepsilon,\mathbf{r})\,G(\varepsilon)$ equals $\chi^{(N)}(\mathbf{r})$ times the Nth divided difference of $G(\varepsilon)$. Moreover, if we let $\omega^{(N)}(\varepsilon,\mathbf{r})$ be a polynomial in energy of (N-1)st degree, its Nth divided difference on the $\epsilon_0, ..., \epsilon_N$-mesh, $\Delta^N\omega^{(N)}(\mathbf{r})/\Delta[0...N]$, will vanish. We have therefore found the following solution for the NMTO set:

$$\chi^{(N)}(\mathbf{r}) = \frac{\Delta^N\phi(\mathbf{r})\,G}{\Delta[0...N]}\left[\frac{\Delta^N G}{\Delta[0...N]}\right]^{-1} = \sum_{n=0}^{N}\phi(\epsilon_n,\mathbf{r})\,L_n^{(N)} = \tag{7}$$

$$\phi(\epsilon_N,\mathbf{r}) + \frac{\Delta\phi(\mathbf{r})}{\Delta[N-1,N]}\left(E^{(N)}-\epsilon_N\right) + ... + \frac{\Delta^N\phi(\mathbf{r})}{\Delta[0...N]}\left(E^{(1)}-\epsilon_1\right)..\left(E^{(N)}-\epsilon_N\right).$$

Here, the second expression may be interpreted as Lagrange interpolation of the energy-dependence of the kinked partial-wave set, but with the weights, $L_n^{(N)}$, being energy-independent *matrices* rather than Nth-degree scalar polynomials in energy. Similarly, the last expression may be interpreted as Newton interpolation (Taylor expansion for a condensed mesh) with the energies substituted by (non-commuting and non-Hermitian) energy-independent matrices, $E^{(M)}$. Using the well-known expression:

$$\frac{\Delta^N G}{\Delta[0...N]} = \sum_{n=0}^{N}\frac{G(\epsilon_n)}{\prod_{m=0,\neq n}^{N}(\epsilon_n-\epsilon_m)} \quad\rightarrow\quad \frac{1}{N!}\left.\frac{d^N G(\varepsilon)}{d\varepsilon^N}\right|_{\epsilon_n},$$

for a divided difference, these matrices are seen to be given by:

$$L_n^{(N)} = \frac{G(\epsilon_n)}{\prod_{m=0,\neq n}^{N}(\epsilon_n-\epsilon_m)}\left[\frac{\Delta^N G}{\Delta[0...N]}\right]^{-1},$$

$$E^{(N)} = \epsilon_N + \frac{\Delta^{N-1}G}{\Delta[0..N-1]}\left[\frac{\Delta^N G}{\Delta[0...N]}\right]^{-1} = \sum_{n=0}^{N}\epsilon_n L_n^{(N)},$$

in terms of the values of the Green matrix on the energy mesh. Note that $\sum_{n=0}^{N} L_n^{(N)}$=1. From the Newton expression (7), we realize that the NMTO equals a kinked partial wave at the same site and with the same angular momentum, plus a smoothing cloud of energy-derivative functions centered at all sites and with all angular momenta (NMTOs with N > 0 are smooth because the kinks $(\mathcal{H}-\varepsilon)\,\phi(\varepsilon,\mathbf{r})\,G(\varepsilon)$ are independent of ε). In the right-hand side of Fig. 1, the solid curve is the MTO with N = 1, the *linear* MTO (LMTO), and the dashed curve is the MTO with N = 0, shown by the solid curve in the left-hand side. Obviously, longer spatial range is the price for spanning wave functions of a wider energy range. This increase of range and smoothness with N, follows from the relation:

$$(\mathcal{H}-\varepsilon_N)\,\chi^{(N)}(\mathbf{r}) = \chi^{(N-1)}(\mathbf{r})\left(E^{(N)}-\varepsilon_N\right), \tag{8}$$

which also shows that the energy matrices are transfer matrices between NMTO sets of different order.

Variational eigenvalue equations: Since from Eq.(6), the NMTO set has errors $\propto \prod_{n=0}^{N}(\varepsilon_i - \epsilon_n)$, solution of the variational eigenvalue equations (4) will yield energies with errors $\propto \prod_{n=0}^{N}(\varepsilon_i - \epsilon_n)^2$. To exploit this, we need the following expressions:

$$\left\langle \chi^{(N)} \left| \mathcal{H} - \epsilon_N \right| \chi^{(N)} \right\rangle = -\left[\frac{\Delta^N G}{\Delta\,[0...N]}\right]^{-1} \frac{\Delta^{2N} G}{\Delta\,[[0..N-1]\,N]} \left[\frac{\Delta^N G}{\Delta\,[0...N]}\right]^{-1}$$

$$\left\langle \chi^{(N)} \mid \chi^{(N)} \right\rangle = -\left[\frac{\Delta^N G}{\Delta\,[0...N]}\right]^{-1} \frac{\Delta^{2N+1} G}{\Delta\,[[0...N]]} \left[\frac{\Delta^N G}{\Delta\,[0...N]}\right]^{-1}.$$

for the Hamiltonian and overlap matrices. Here, $\Delta^{M+N+1}G/\Delta\,[[0..M]\,N]$ is the (M + N + 1)th derivative of that polynomial of degree M + N + 1 which takes the values $G_0, ..., G_N$ at the N + 1 mesh points and the values $\dot{G}_0, .., \dot{G}_M$ of the first-derivative at the first M + 1 points. Note that this Hermite interpolation of $G(\varepsilon)$ is not supposed to approximate $G(\varepsilon)$, which usually has poles inside the mesh; the physical quantities are *ratios* of energy derivatives of such polynomial 'approximations'. The Hamiltonian and overlap matrices may be expressed in terms of the values and first energy derivatives at the mesh of the smooth function $K(\varepsilon) \equiv G(\varepsilon)^{-1}$, but as N increases, these expressions become increasingly complicated.

As a first example, we consider the simplest possible 1×1 Green matrix, $G(\varepsilon) = \sum_j (\varepsilon - \varepsilon_j)^{-1}$, which is that of a single, normalized kinked partial wave: The variational energy relative to ϵ_N can be worked out to be:
$\frac{\Delta^{2N} G}{\Delta[[0..N-1]N]} \Big/ \frac{\Delta^{2N+1} G}{\Delta[[0...N]]} = \sum_j (\varepsilon_j - \epsilon_N)^{-1} \prod_{n=0}^{N-1} (\varepsilon_j - \epsilon_n)^{-2} \Big/ \sum_j \prod_{n=0}^{N} (\varepsilon_j - \epsilon_n)^{-2}$, and the deviation from an exact result, $\varepsilon_i - \epsilon_N$, is therefore $\sum_{j \neq i} (\varepsilon_j - \epsilon_N) \prod_{n=0}^{N} (\varepsilon_i - \epsilon_n)^2 / (\varepsilon_j - \epsilon_n)^2$, to leading order. This is in accord with the opening statement of this subsection. Fig. 2 shows how for the two-level system $G(\varepsilon) = \frac{1}{\varepsilon} + \frac{1}{\varepsilon - 1}$, this variational energy switches from 0 to 1 as the center, x, of the mesh sweeps from –1 to +2. The various curves refer to N = 0, 1, 2, and 4. For N > 0, we used meshes of total width 0.4. We see that the switching curves sharpen up as N increases, and that good results are obtained already with N = 1, the chord-LMTO.

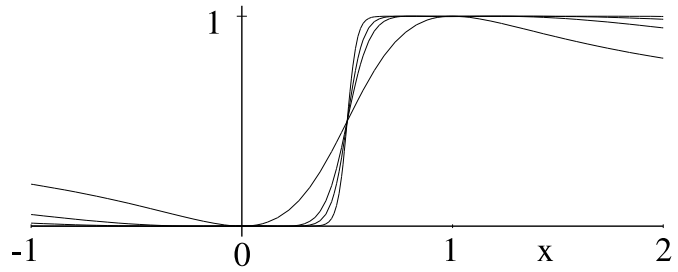

Figure 2: *Variational energy-estimates for a two-level model (ε_i = 0, 1) using single NMTOs with N = 0, 1, 2, and 4 as functions of the position, x, of the center of the energy mesh.*

Density-functional calculations: In Fig. 3 we show for GaAs the LDA valence and conduction bands, 18 of which fall in the 35 eV-range displayed. The solid curves are the exact bands and the dotted curves are the bands calculated variationally using a basis of Ga sp^3d^5 and As $sp^3d^5f^7$ quadratic muffin-tin orbitals (QMTOs) with the three energies indicated in the right-hand panel. The good accuracy achieved with this basis of merely 25 orbitals/cell demonstrates the power of

our method. Note that even for this large energy range, no radial quantum numbers are needed. In most cases (self-consistency iterations) one merely needs to describe the *occupied* states, which for GaAs are the five semi-core Ga $3d$ bands at -15 eV, the As $4s$-like band around -11 eV, and the three valence bands of dominant Ga $4s4p$ and As $4p$ characters extending from -7 to 0 eV. With a minimal Ga sp^3d^5 As sp^3 NMTO set, we find typical accuracies in the sum of the one-electron energies of 50 and 5 meV/GaAs respectively for LMTOs (ϵ_0 $\approx$-15 eV, -5 $< \epsilon_1 <$ -2 eV) and QMTOs ($\epsilon_0 \approx$ -15 eV, $\epsilon_1 \approx$ -11 eV, -5 $< \epsilon_2 <$ -2 eV).

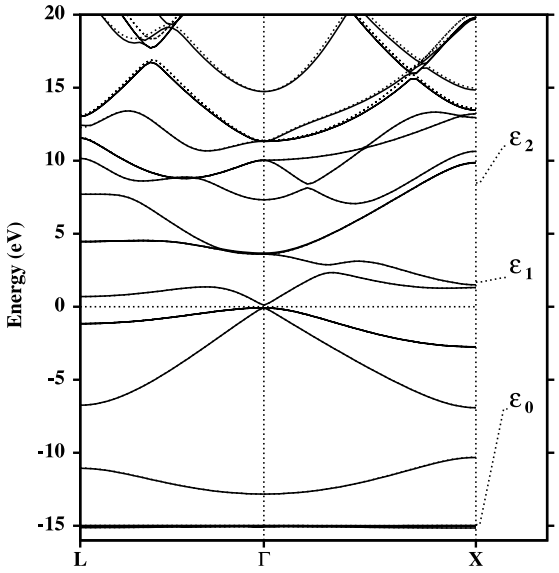

Figure 3: *Band structure of GaAs in the LDA, calculated with the variational QMTO method (dashed), as compared with the exact KKR result (solid).*

Wannier-like orbitals: For cuprate high-temperature superconductors, one needs a one-band Hubbard Hamiltonian with realistic, material-dependent parameters. The conduction band obtained from angle-resolved photoemission, or with the LDA (Fig. 4), has anti-bonding O p_x−Cu $d_{x^2-y^2}$−O p_y character, but it crosses, or hybridizes with a multitude of other bands below the Fermi level ($\sim$-0.7 eV), so that its Wannier function is long ranged and depends on irrelevant details. Rather than the Wannier function, one therefore wants an exponentially decaying orbital, which describes the band in a range around the Fermi level. The dotted band in Fig. 4 results from an N = 3 variational calculation, in which only the Cu $d_{x^2-y^2}$-channel was taken as active. It is seen to give a superb description of the conduction band in the regions where this band is isolated, including the extended saddle-point at X, and a smooth interpolation below -1.4 eV where the band is hybridized. The Fourier transform yields the hopping integrals.

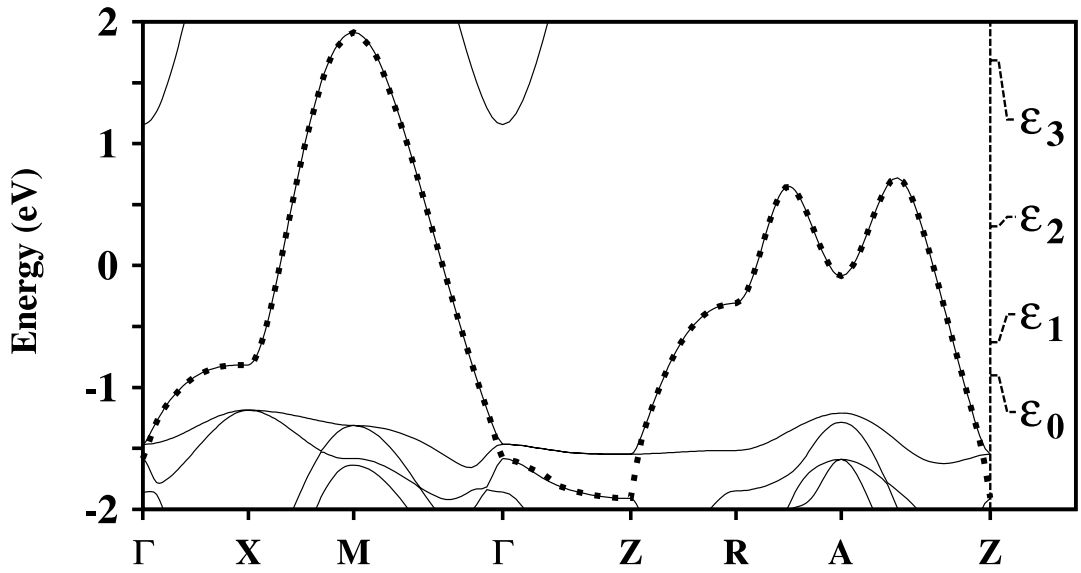

Figure 4: *Band structure of $CaCuO_2$ with a 7^0-buckle, calculated in the LDA with a single, Bloch Cu $d_{x^2-y^2}$ CMTO (dotted) compared with the full band structure (solid).*

For calculating the Coulomb interaction and, more generally, for multiband model Hamiltonians, minimal orthonormal bases are required. With NMTOs, there is an efficient way to generate orthonormal sets, which goes via sets of so-called *nearly orthonormal* NMTOs. Before we indicate how this works, we recall that Löwdin orthonormalization is: $\check{\chi}(\mathbf{r}) = \chi(\mathbf{r}) \langle \chi \mid \chi \rangle^{-1/2}$, where the $\chi(\mathbf{r})$'s are normalized and where the matrix $\langle \chi \mid \chi \rangle^{-1/2}$ is obtained by Taylor-expansion in the non-orthonormality $1 - \langle \chi \mid \chi \rangle$, which is therefore required to be small. We also state, without proof, that the NMTO set, $\hat{\chi}^{(N)}(\mathbf{r})$, derived from the set, $\hat{\phi}(\varepsilon, \mathbf{r}) = \phi(\varepsilon, \mathbf{r}) \hat{T}(\varepsilon)$, of transformed kinked partial waves, is a linear transformation of the original set, $\chi^{(N)}(\mathbf{r})$, and is given by hatted version of expressions (7). It now turns out to be a simple matter to find the transformation, $\hat{T}(\varepsilon)$, which makes the sets $\hat{\chi}^{(M)}(\mathbf{r})$ nearly orthonormal, in the sense that $\left\langle \hat{\chi}^{(M-1)} \mid \hat{\chi}^{(M)} \right\rangle = 1$ for $1 \leq M \leq N$, and for instance $\hat{\phi}(\epsilon_0, \mathbf{r}) = \hat{\chi}^{(0)}(\mathbf{r})$ is normalized. In such a representation, $\left\langle \hat{\chi}^{(N)} \mid \hat{\chi}^{(N)} \right\rangle$ is sufficiently close to the unit matrix that the non-orthonormality can be neglected, and if not, Löwdin orthonormalization will converge fast. The added bonus of a nearly orthonormal representation is that its energy matrices are Hamiltonians, as may be seen from the relation: $\hat{E}^{(M)} - \epsilon_M = \left\langle \hat{\chi}^{(M)} \mid \hat{\chi}^{(M-1)} \right\rangle^{-1} \left\langle \hat{\chi}^{(M)} \left| \mathcal{H} - \epsilon_M \right| \hat{\chi}^{(M)} \right\rangle$, derived from Eq.(8).

Generating the kink matrix: Having seen that both the NMTOs and the Hamiltonian and overlap matrices are expressed in terms of *one* matrix, $G(\varepsilon) \equiv K(\varepsilon)^{-1}$, let us finally indicate how the kink matrix is generated. The elements with $R \neq R'$ of the *bare* structure matrix, $B^0_{R'L',RL}(\varepsilon) \equiv \sum_{l''} 4\pi i^{-l+l'-l''} C_{LL'l''} \kappa n_{l''}(\kappa |\mathbf{R} - \mathbf{R}'|) Y^*_{L''}\left(\widehat{\mathbf{R} - \mathbf{R}'}\right)$, specify how the spherical waves, $n_l(\kappa r_R) Y_L(\hat{r}_R)$, are expanded in regular spherical waves, $j_{l'}(\kappa r_{R'}) Y_{L'}(\hat{r}_{R'})$. The expansions of the *screened* spherical waves are specified by the screened structure matrix, $B^\alpha(\varepsilon)$, which is obtained by matrix inversion of $B^0(\varepsilon) + \kappa \cot \alpha(\varepsilon)$. Here, $B^0_{RL',RL}(\varepsilon) \equiv 0$ and $\kappa \cot \alpha(\varepsilon)$ is a diagonal matrix with $\alpha_{RL}(\varepsilon)$ being the hard-

sphere phase shift $[\tan\alpha_{Rl}(\varepsilon) \equiv j_l(\kappa a_R)/n_l(\kappa a_R)]$ if the channel is active, and the real phase shift $\eta_{Rl}(\varepsilon)$ if the channel is inactive. With appropriate division into active and inactive channels, $B^\alpha(\varepsilon)$, defined via $B^\alpha(\varepsilon)^{-1} \equiv B^0(\varepsilon)^{-1} + \kappa^{-1}\tan\alpha(\varepsilon)$, has short spatial range and no poles in the energy-range of interest. Finally, the kink matrix is $K(\varepsilon) = -[\kappa n(\kappa a)]^{-1}[B^\alpha(\varepsilon) + \kappa\cot\eta^\alpha(\varepsilon)][\kappa n(\kappa a)]^{-1}$, where $\eta^\alpha(\varepsilon)$ is the real phase shift in the medium of hard a-spheres $[\tan\eta^\alpha(\varepsilon) \equiv \tan\eta(\varepsilon) - \tan\alpha(\varepsilon)]$.

Overlapping MT-wells: In closing, a point of considerable practical importance. The KKR and NMTO formalisms hold not only for straight MT-potentials, but for superpositions of *overlapping* MT-wells, to first order in the potential-overlap. In order to exploit this, we need to use kinked partial waves defined as in the left-hand part of Fig. 1: $\phi_{RL}(\varepsilon,\mathbf{r}) \equiv [\varphi_{Rl}(\varepsilon,r_R) - \varphi^o_{Rl}(\varepsilon,r_R)]\,Y_L(\hat{r}_R) + \psi_{RL}(\varepsilon,\mathbf{r})$. Here, $\varphi(\varepsilon,r)$ (dot-dashed) is the radial solution for the central MT-well, which extend to the radius $s\,(>a)$, and $\varphi^o(\varepsilon,r)$ (dotted) is the phase-shifted wave proceeding smoothly inwards from s to the central a-sphere, where it is matched with a kink to the screened spherical wave ψ (dashed). Radial overlaps of up to 30% may be treated without changing the formalism, and overlaps up to 60% may be treated if a simple kinetic-energy correction is included. The NMTOs generated from such potentials are accurate for all cases we have considered so far.